[1] **Vinamra K. Govil***

[2] **S. M. Tripathi**

[3] **Kuldeep Sahay**

Performance Evaluation of PMSG-Wind Energy Conversion System with Integrated DSTATCOM Functionality for Enhanced Grid Power Quality: A Real-time Simulation Approach

Journal of Electrical Systems

Abstract: This paper presents a dynamic performance evaluation of a permanent magnet synchronous generator (PMSG)–wind energy conversion system (WECS) with integrated DSTATCOM functionality. The system employs back-to-back voltage source converters (VSCs), where the grid-side VSC not only transfers power but also compensates for harmonics and reactive power, enhancing grid power quality. The control strategy utilizes field-oriented control for PMSG and indirect current control for the VSC to ensure unity power factor and harmonic suppression at the Point of Common Coupling (PCC). Real-time simulations using the Typhoon HIL 604 simulator are conducted for two scenarios: (1) gradual wind speed variation and (2) sudden load reduction. The results demonstrate effective PMSG speed tracking, stable grid voltage, reduced harmonic distortion (THD < 5%), and smooth power adaptation, confirming the system's capability to improve grid stability and power quality under varying wind and load conditions.

Keywords: DSTATCOM, harmonic compensation, power quality, PMSG, real-time simulation, Typhoon HIL, wind energy conversion system.

I. INTRODUCTION

The rising integration of renewable energy sources, especially wind energy, into modern power grids poses challenges to power quality, grid stability, and reliable energy integration. Among these sources, permanent magnet synchronous generator (PMSG)–wind energy conversion systems (WECS) have gained prominence due to their high efficiency, direct-drive configuration, and improved reliability [1]. However, the fluctuating nature of wind speeds leads to variable power output, which can result in voltage instability, harmonic distortion, and poor power factor in the grid [2].

To mitigate these challenges, modern power systems increasingly adopt multifunctional power electronic converters, such as voltage source converters (VSC), to serve dual roles: facilitating efficient power transfer and providing grid support functionalities like harmonic compensation and reactive power management. By integrating distributed static compensator (DSTATCOM) functionality [3–5] within the grid-side VSC of a PMSG-based WECS, it is possible to significantly enhance grid power quality while ensuring stable system operation, even under varying wind and load conditions. The three-phase four-wire configuration further ensures effective neutral current compensation and handling of unbalanced loads [6].

The integration of WECS poses significant challenges to power quality and grid stability, necessitating the use of advanced control strategies. Studies have highlighted the critical role of DSTATCOM in mitigating grid issues such as voltage sags, swells, and harmonic distortions, while enhancing reactive power compensation and voltage regulation [7]. Additionally, the optimal tuning of PI controllers is essential for achieving precise control over active and reactive power, reducing system oscillations, and maintaining voltage stability in PMSG-WECSs [8]. Advanced converter control methods, including vector control and direct torque control, offer dynamic power decoupling and effectively reduce harmonic distortion, improving system performance, as discussed in [9]. For handling nonlinear loads, intelligent controllers have been introduced to adaptively manage harmonic distortion

[1] *Corresponding author: Research Scholar, Dr. A. P. J. Abdul Kalam Technical University, Lucknow – 226031 (U.P.), India; vinamragovil1985@gmail.com

[2]Power & Energy Research Centre, Electrical Engineering Department, Kamla Nehru Institute of Technology, Sultanpur – 228118 (U.P.), India; mani@knit.ac.in

[3]Electrical Engineering Department, Institute of Engineering & Technology, Lucknow – 226021 (U.P.), India; kuldeep.sahay@ietlucknow.ac.in

and significantly improve power quality [10]. Nonlinear adaptive control mechanisms are further proposed to maintain optimal performance under fluctuating operational conditions, enhancing both power factor and frequency regulation [11]. Moreover, real-time state estimation techniques play a crucial role in detecting and correcting transient disturbances, thereby ensuring continuous voltage stability [12]. The control of torsional oscillations and power damping is also key to maintaining overall system stability and improving power flow management, as explored in [13]. The studies [14–26] emphasize the importance of integrating advanced control and compensation techniques to enhance power quality, mitigate harmonics, and ensure stable grid performance in PMSG–WECSs.

This paper proposes and analyzes a grid-connected PMSG–WECS with integrated DSTATCOM functionality aimed at improving grid power quality. The system is designed not only to generate and deliver clean energy but also to actively participate in harmonic suppression, and reactive power compensation. Through real-time simulations, the proposed system's performance is evaluated under varying wind speeds and load disturbances, demonstrating its effectiveness in ensuring grid power quality.

The key contributions of this work are threefold: (1) the development of a control strategy that combines field-oriented vector control for the PMSG and indirect current control for the grid-side VSC, (2) a detailed real-time simulation-based analysis of the system's dynamic response to wind speed variations and sudden load changes, and (3) validation of the system's ability to maintain total harmonic distortion (THD) of the grid current within IEEE standards (<5%) while ensuring unity power factor. The results demonstrate the potential of integrating DSTATCOM functionality into wind energy systems for seamless and reliable renewable energy integration into modern grids.

This paper is structured as follows: Section II outlines the system configuration and modeling approaches. Section III provides a detailed explanation of the control methodology employed. Section IV presents and analyzes the simulation results, highlighting system performance. Section V concludes with a summary of key findings and implications.

II. System Configuration and Modeling

The proposed system, as depicted in Figures 1 and 2, consists of a grid-connected PMSG–WECS with a two-level back-to-back converter configuration. The converter at the machine-side (MSC) controls the PMSG, while the converter at the grid-side (VSC) functions as both a power transfer interface and a DSTATCOM for grid support.

A. Wind Turbine

The mechanical power output P_m of the wind turbine is determined by

$$P_m = \frac{1}{2}\left(\rho C_p A V_\omega^3\right) \tag{1}$$

where ρ represents the air density (kg/m³); A denotes the swept area of the blades (m²); V_ω indicates the wind speed (m/s); and C_p stands for the power coefficient.

$$C_p = 0.73\left[\frac{151}{\lambda_i} - 13.2 - 0.58\theta - 0.002\theta^{2.14}\right]\exp\left[-\frac{18.4}{\lambda_i}\right] \tag{2}$$

$$\frac{1}{\lambda_i} = \frac{1}{\lambda + 0.08\theta} - \frac{0.035}{1+\theta^3} \tag{3}$$

$$\lambda = \frac{\omega_r R}{V_\omega} \tag{4}$$

where λ denotes the tip-speed-ratio (TSR), θ indicates the pitch angle, R is the radius of the turbine blades, and ω_r represents the mechanical rotor speed of the PMSG.

B. PMSG

The surface mounted PMSG is modeled in the *d-q* reference frame. The voltage equations are

$$V_{ds} = L_s\left(\frac{d}{dt} i_{ds}\right) + R_s i_{ds} - \omega_s L_s i_{qs} \tag{5}$$

$$V_{qs} = L_s\left(\frac{d}{dt}i_{qs}\right) + R_s i_{qs} + \omega_s L_s I_{ds} + \omega_e \lambda_m \quad (6)$$

The generator torque equation can be written as

$$T_e = 0.75\left(P\lambda_m i_{qs}\right) \quad (7)$$

where V_{ds} and V_{qs} are the *d*-*q* axes stator voltages; i_{ds} and i_{qs} are the *d*-*q* axes stator currents; R_s is the stator resistance; L_s is the stator inductance; λ_m is the rotor flux; ω_e is the electrical speed of the PMSG; and P is the number of poles of the PMSG.

C. Converter Interface

The proposed system features a two-level back-to-back VSC setup comprising a MSC and a grid-side VSC. The MSC connects to the PMSG to manage the generator's power output, while the VSC interfaces with the grid, fulfilling dual roles of power transfer and functioning as a DSTATCOM to compensate for harmonics and reactive power to enhance grid power quality.

D. Point of Common Coupling (PCC)

At the PCC, the system interfaces with a diverse range of loads, including both single-phase and three-phase configurations. These loads encompass both linear and non-linear types.

E. Power Grid

The equations for the grid voltages are expressed as follows

$$e_{dg} = L_g\left(\frac{d}{dt}i_{dg}\right) + R_g i_{dg} - \omega_g L_g i_{qg} + \nu_{dg} \quad (8)$$

$$e_{qg} = L_g\left(\frac{d}{dt}i_{qg}\right) + R_g I_{qg} + \omega_g L_g i_{dg} + \nu_{qg} \quad (9)$$

where, e_{dg} and e_{qg} denote the components of grid voltage along the *d*-axis and *q*-axis, respectively; R_g represents the coupling resistance; L_g stands for coupling inductance; ν_{dg} and ν_{qg} are the *d*-axis and *q*-axis grid-side VSC voltage components, respectively; and ω_g signifies the grid angular frequency.

III. Control Methodology

The PMSG control is implemented through field-oriented vector control (FOC), utilizing a PI controller for speed regulation in the outer loop and a hysteresis controller for generator current control in the inner loop. For the grid-side VSC, an indirect current control scheme is employed, with a PI controller regulating the DC link voltage and a hysteresis controller managing the VSC current. This control scheme effectively addresses harmonics, compensates for non-linear loads at the PCC, and ensures efficient power transfer to the grid, thereby enhancing both the quality and stability of the grid power.

A. MSC Control

In the proposed WECS, the control of the PMSG is crucial for optimizing power extraction and ensuring efficient operation. The control strategy for the MSC, as illustrated in Figure 1, is designed to maximize energy capture from the wind while maintaining stable generator performance. To achieve optimal power generation, the generator speed is controlled to follow the maximum power point (MPP). The tip-speed ratio (TSR) control algorithm is used for maximum power point tracking (MPPT) to determine the optimal generator speed by taking into account the wind speed and turbine characteristics. The TSR control algorithm provides a reference speed (ω^*_e) that the generator should aim to achieve to operate at the MPP. The PI controller takes the difference between the reference generator speed (ω^*_e) and the actual generator speed (ω_e) to calculate the required reference torque (T^*_e). This PI controller adjusts the generator's torque to minimize the speed error, ensuring the generator operates at its optimal point. The reference torque is given by the equation

$$T^*{}_e = K_{ps}\left(\frac{pT_{is}+1}{pT_{is}}\right)\left(\omega^*{}_e - \omega_e\right) \quad (10)$$

where T_{is} stands for integral time constant and K_{ps} stands for the proportional gain of PI speed controller.

$$i^*{}_{qs} = (4/3)\left(\frac{T^*{}_e}{P\lambda_m}\right) \quad (11)$$

The *q*-axis reference generator current component is determined from the reference torque using equation (11). This component controls the generator's torque production and is crucial for achieving the desired mechanical output. In contrast, the *d*-axis reference generator current component is set to zero to optimize performance. Setting the *d*-axis generator current to zero allows the system to achieve maximum torque with minimal current. This approach enhances efficiency by reducing electrical losses. The *d-q* axes reference generator currents are transformed into *abc* reference currents (I^*_{sabc}). After comparing the actual currents (I_{sabc}) with the reference currents (I^*_{sabc}), the error is fed into the hysteresis controller, which regulates the generator current and generates the switching signals for the MSC. Choosing the appropriate hysteresis band ensures that the switching frequency of the MSC remains within its allowable range.

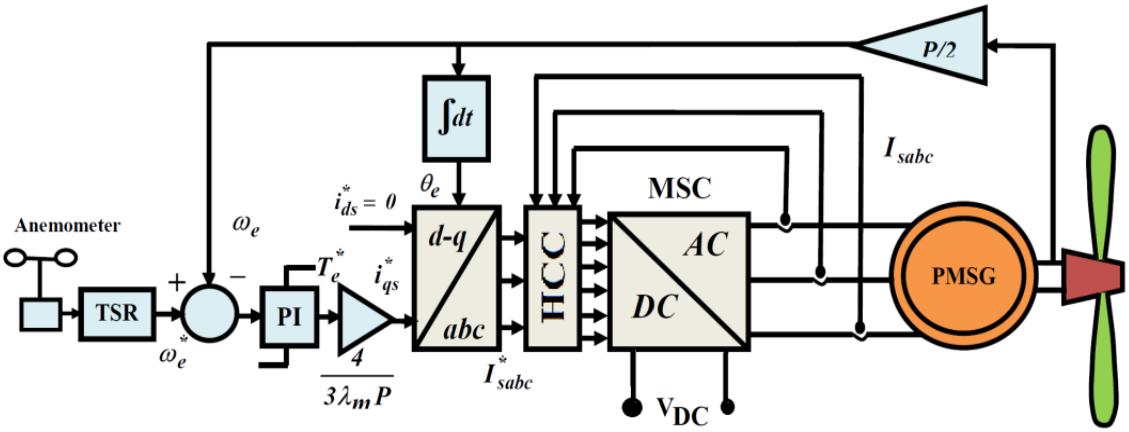

Fig.1. The control for MSC of proposed grid-connected PMSG–WECS.

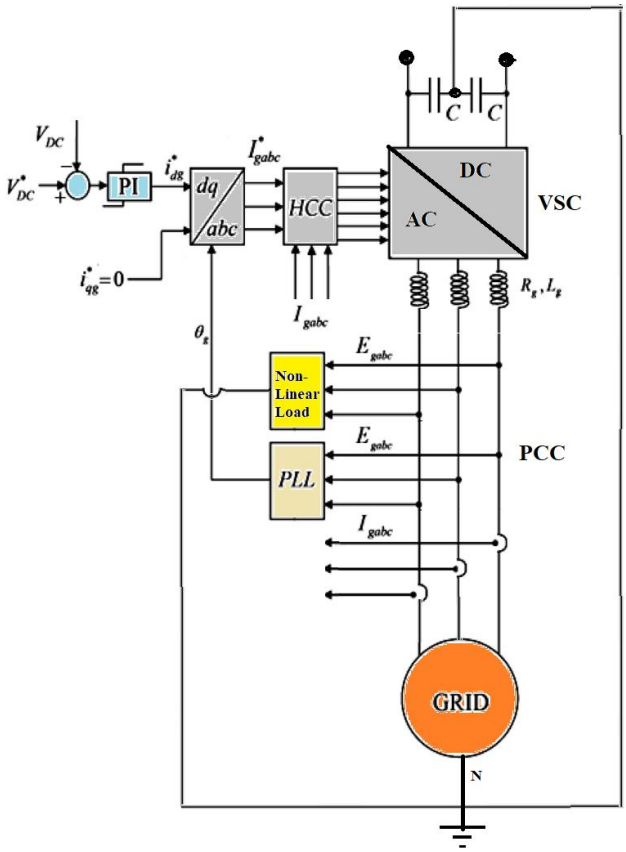

Fig.2. The indirect current control scheme for the grid-side VSC with DSTATCOM functionality.

The machine-side control, as illustrated in Figure 1, regulates the generator's speed and torque effectively. By maintaining the generator at or near its MPP, the MSC ensures that the WECS operates efficiently under varying wind conditions.

B. Grid-side VSC Control

In the proposed WECS, the grid-side VSC performs two key functions: it regulates the DC-link voltage and compensates for harmonics and reactive power, thereby improving power quality at the PCC. The VSC control strategy is implemented using a two-loop cascaded control system designed to handle fluctuating wind power and grid disturbances efficiently as depicted in Figure 2. The main goal of the outer control loop is to keep the DC-link voltage stable. This helps maintain the power balance between the wind power generated and the power transferred to the grid. The error between the reference DC-link voltage ($V_{DC}{}^{*}$) and the actual DC-link voltage (V_{DC}) is processed by a PI controller, which produces the reference direct-axis grid current ($i^{*}{}_{dg}$). This current manages the active power exchange between the WECS and the grid and is defined as

$$i^{*}{}_{dg} = K_{pv}\left(\frac{1+pT_{iv}}{pT_{iv}}\right)\cdot\left(V_{DC}{}^{*} - V_{DC}\right) \tag{12}$$

where T_{iv} stands for integral time constant, K_{pv} stands for the proportional gain of the DC link voltage PI controller.

The inner current loop plays a critical role in managing the grid-side currents to ensure effective harmonic suppression and reactive power compensation. The VSC actively compensates for the reactive power and harmonic currents generated by nonlinear loads connected at the PCC. By doing so, it ensures that the grid current predominantly consists of the fundamental active current component, thereby enhancing power quality and maintaining operation at a unity power factor (UPF). Consequently, the grid is relieved from supplying reactive or harmonic currents, leading to a sinusoidal grid current and improved power quality. To achieve UPF, the reference quadrature-axis grid current ($i^{*}{}_{qg}$) is set to zero, as the reactive power should be fully compensated by the VSC. The active power supplied to the grid is controlled by the direct-axis current component (i_{dg}), which also regulates the DC-link voltage.

This control scheme utilizes only three current sensors and four voltage sensors to monitor voltage and current, enabling the grid-side VSC to function effectively without needing detailed information about the grid-side VSC current and load current profiles. The proposed control ensures that the grid currents remain sinusoidal, regardless of the non-linear nature of the load, effectively reducing the THD at the PCC.

Fig. 3. Typhoon HIL 604 based real-time simulation setup.

IV. Real-time Simulation Results

The proposed PMSG–WECS, with integrated DSTATCOM functionality, is rigorously evaluated through detailed real-time simulations. The simulation setup, as illustrated in Fig. 3, is implemented using the Typhoon HIL 604 real-time simulator, ensuring high-fidelity testing and analysis. The system parameters utilized for this real-time simulation are outlined in Appendix, reflecting practical operating conditions. Results obtained from the mixed-signal oscilloscope provide clear evidence of the system's capability to maintain robust power quality and grid stability under varying conditions. The data showcases the effectiveness of the control strategy in mitigating harmonics, ensuring reactive power compensation, and stabilizing voltage levels even in the presence of fluctuating wind speeds and non-linear loads.

A. Performance Evaluation

The performance evaluation focuses on two cases: gradual wind speed variation (9 m/s to 11 m/s) and sudden load reduction at rated wind speed (11 m/s). These cases highlight the system's adaptability and power quality management under dynamic conditions.

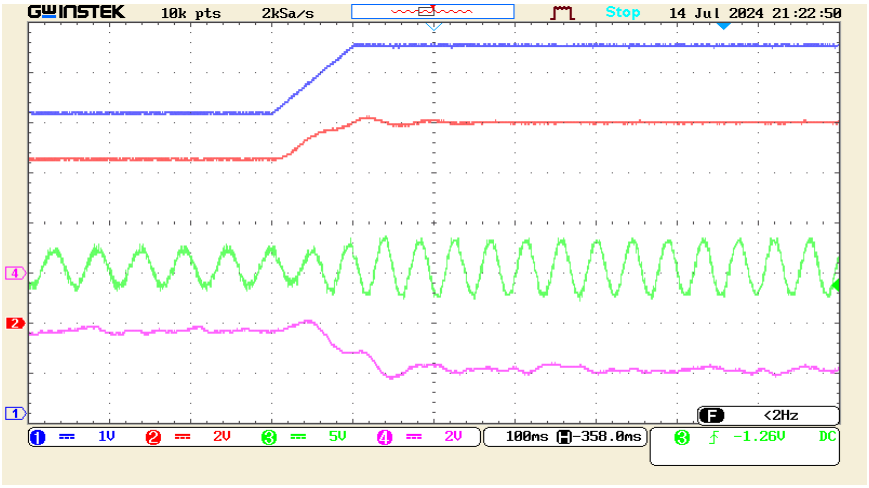

Fig. 4. Real time performance of MSC control when wind speed gradually changing from 9 m/s to 11 m/s—CH1: wind speed (1.5 m/s per div—blue trace), CH2: rotor speed (6 rad/s per div—red trace), CH3: generator current (25 A per div—green trace), CH4: generated power (4000W per div—magenta trace).

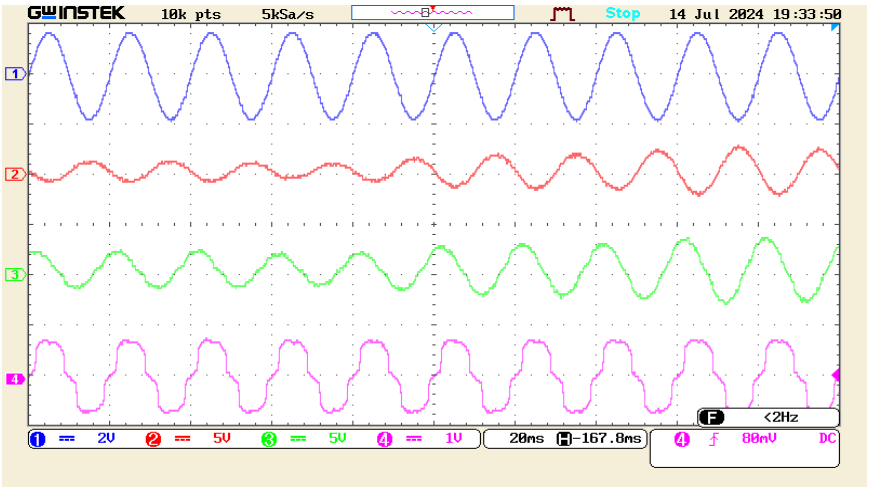

Fig. 5. Real time performance of proposed WECS when wind speed gradually changing from 9 m/s to 11 m/s at fixed linear/nonlinear load connected at PCC—CH1: voltage at PCC (400V per div—blue trace), CH2: source (grid) current (25 A per div—red trace), CH3: VSC current (25 A per div—green trace), CH4: load current (5A per div—magenta trace).

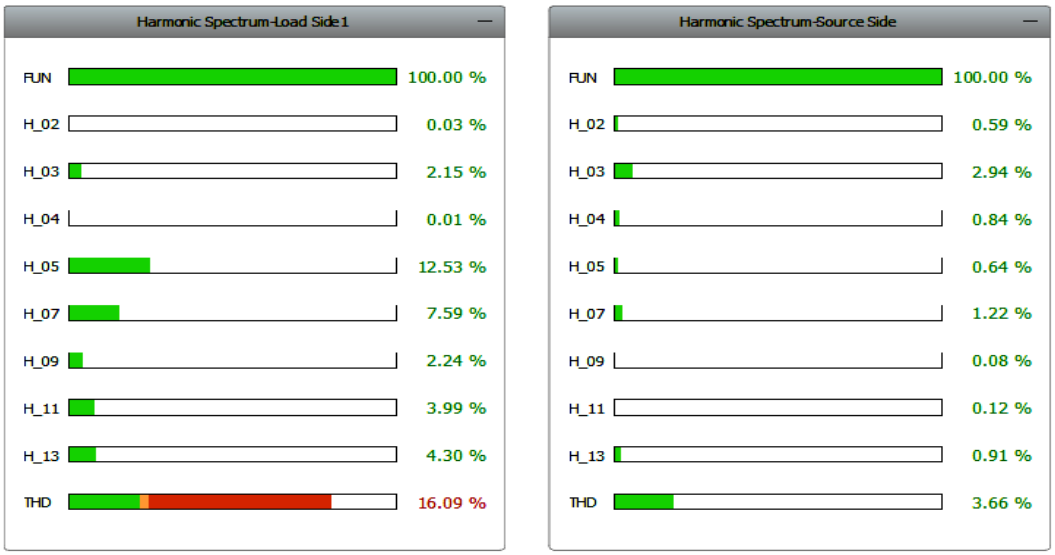

(a)

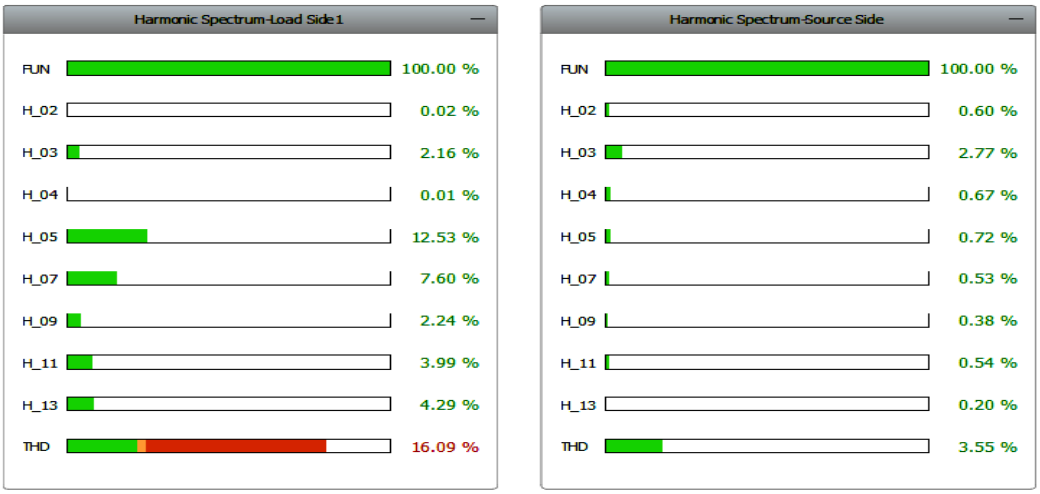

(b)

Fig. 6. Total harmonic distortion (THD) of—(a) load and source (grid) currents (Phase–*a*) at wind speed of 9 m/s; (b) load and source (grid) currents (Phase–*a*) at rated wind speed of 11 m/s.

Case 1: Gradual Wind Speed Variation (9 m/s to 11 m/s) —As the wind speed increases gradually from 9 m/s to 11 m/s, the PMSG rotor speed adjusts smoothly from about 19.6 rad/s to 24 rad/s, demonstrating effective tracking of the reference speed set by the MPPT algorithm (see Fig. 4). This adjustment ensures optimal power generation in response to changing wind conditions, accompanied by a corresponding increase in PMSG stator current. The grid-side VSC, operating as a DSTATCOM, plays a crucial role in maintaining power quality. Despite the gradual change in wind speed, the grid-side VSC effectively compensates for harmonics and reactive power, ensuring that the grid current remains sinusoidal (Fig. 5). The THD of the grid-injected current remains consistently below 5%, adhering to IEEE standards, while the load current THD is higher at 16.09% due to the presence of non-linear loads (Fig. 6). This performance underscores the grid-side VSC's capability to mitigate harmonic distortion and enhance overall grid power quality.

Case 2: Sudden Load Reduction at Rated Wind Speed (11 m/s)—During a sudden load reduction while operating at the rated wind speed of 11 m/s, the system exhibits exceptional adaptability. The grid-side VSC promptly adjusts its output, ensuring that the grid current remains sinusoidal and the grid voltage stays stable (see Fig. 7(a)). The current injected into the grid rapidly adapts to the load change, preserving sinusoidal waveforms and maintaining unity power factor. This quick response is made possible by the indirect current control scheme, which effectively regulates the grid current even under sudden load variations. The DC link voltage remains steady

at 900 V, demonstrating the system's stability and precise voltage regulation (see Fig. 7(b)). Despite the abrupt load changes, the neutral current on the grid side stays near zero, showcasing the system's efficient handling of load imbalances and minimal impact on the grid (see Fig.7). Additionally, the THD of the load current reduces to 12.69% after the load reduction, while the THD of the grid current remains well within the 5% limit, highlighting the system's capability to manage dynamic conditions effectively (see Fig. 8).

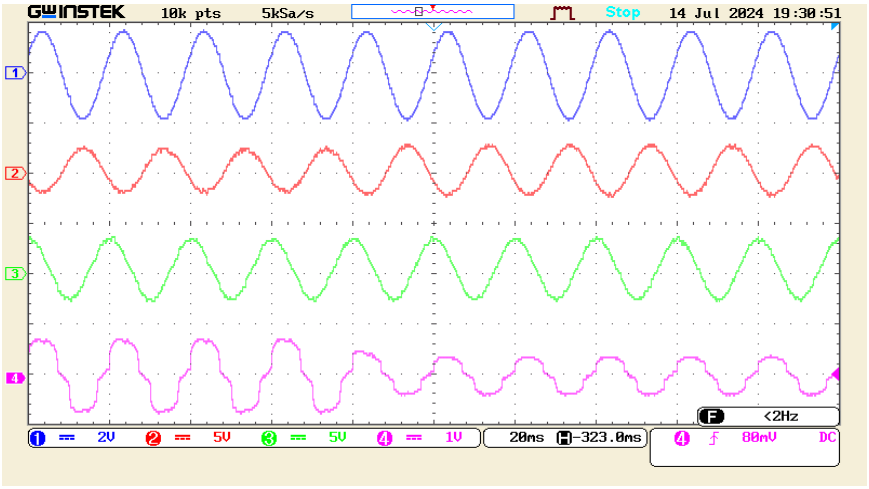

(a)

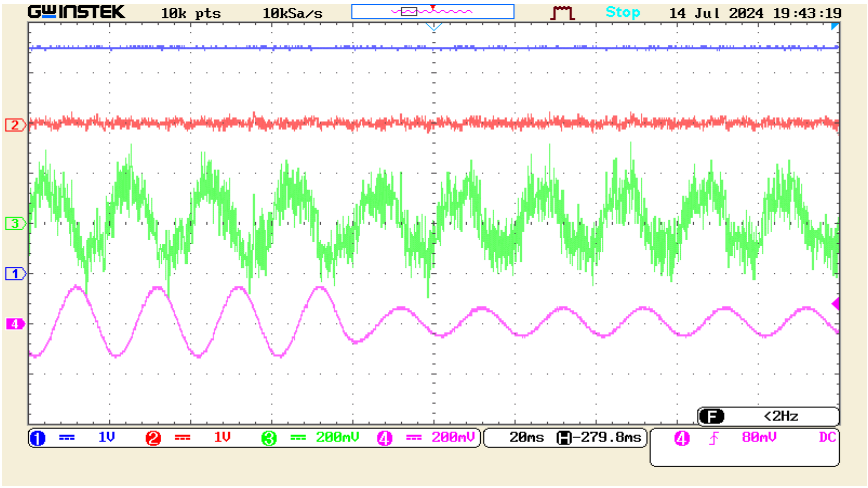

(b)

Fig. 7. Real time performance of proposed WECS under reduced load condition—(a) CH1: voltage at PCC (400V per div—blue trace), CH2: source/grid current (25 A per div—red trace), CH3: VSC current (25 A per div—green trace), CH4: load current (5A per div—magenta trace); (b) CH1: DC link voltage (200V per div—blue trace), CH2: source (grid) neutral current (5 A per div—red trace), CH3: VSC neutral current (1 A per div—green trace), CH4: load current (1A per div—magenta trace).

B. Power Dynamics and System Performance

The power dynamics and overall system performance are critically assessed through Figure 9, which illustrate the behavior of active and reactive power under varying operational conditions. As the wind speed increases from 9 m/s to 11 m/s, the PMSG generates more power to match the increased wind energy input. The grid-side VSC efficiently manages this power transfer, ensuring the active power injected into the grid remains stable and in line with available wind power. The grid-side VSC also adjusts reactive power to stabilize grid voltage and maintain unity power factor, underscoring its dual role in enhancing power quality and facilitating efficient power transfer. In the event of a sudden load reduction at the rated wind speed of 11m/s, the system demonstrates its robustness in managing rapid changes in power demand. The grid-side VSC promptly adjusts its reactive power output to compensate for the decreased load, thereby stabilizing the grid voltage. Concurrently, the active power injected into the grid increases due to the reduced load at the PCC. This highlights the system's robustness in managing dynamic power flows while preserving grid power quality. The consistent DC link voltage at 900 V (see Fig. 7(b))

further emphasizes the system's stability and ability to handle variations in wind speed and load conditions, ensuring reliable grid integration.

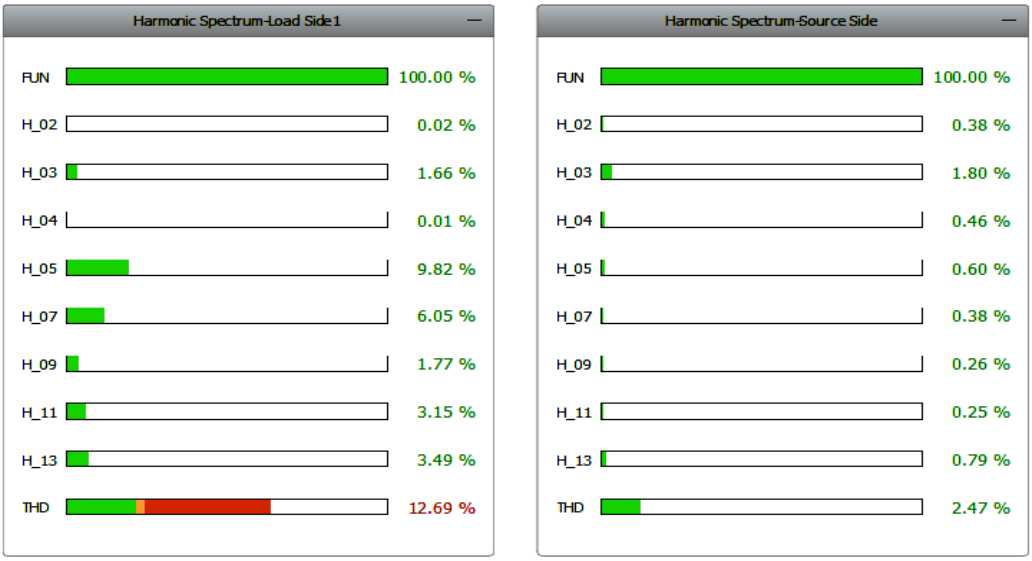

Fig. 8. THD of load and source (grid) currents (Phase-a) under reduced load condition.

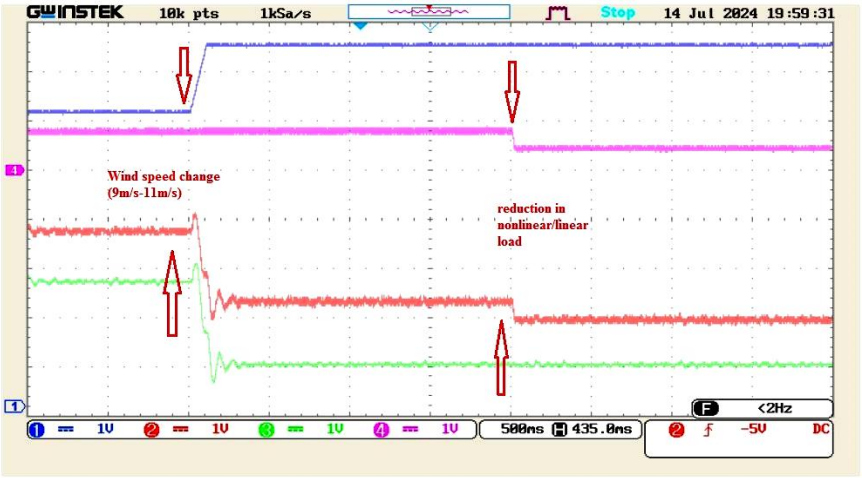

(a)

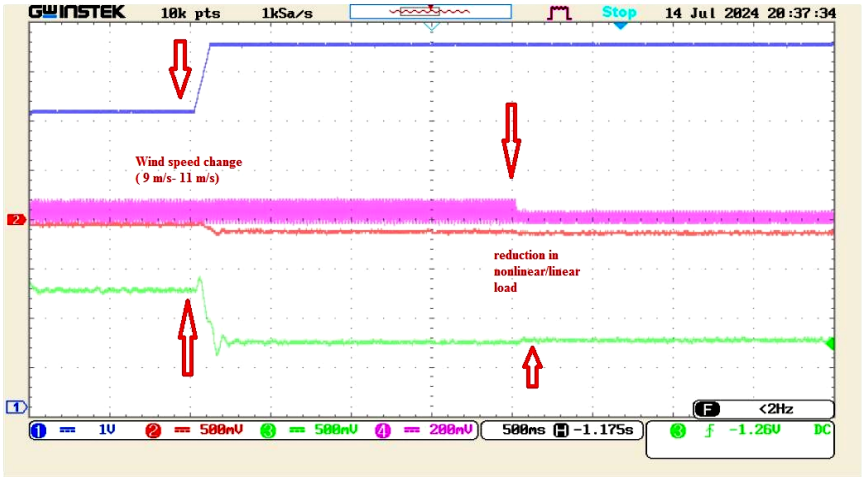

(b)

Fig. 9. Power dynamics and system performance under both varying wind speed and reduced load conditions—(a) active power dynamics: CH1: wind speed (1.5 m/s per div—blue trace), CH2: grid active power (4000 W per div—red trace), CH3: VSC

active power (4000W per div—green trace), CH4: load active power (4000W per div—magenta); (b) reactive power dynamics: CH1: wind speed (1.5 m/s per div—blue trace), CH2: grid reactive power (4000 W per div—red trace), CH3: VSC reactive power (4000W per div—green trace), CH4: load reactive power (4000W per div—magenta trace).

C. Discussion

The real-time simulation results validate the effectiveness of integrating DSTATCOM functionality into the grid-side VSC of PMSG–WECS. The system successfully maintains power quality and stability under gradual and sudden changes in wind speed and load, respectively. This performance is attributed to the advanced control strategies employed. The field-oriented vector control for the PMSG ensures precise rotor speed regulation and optimal power extraction, while the indirect current control for the grid-side VSC efficiently handles harmonic compensation and reactive power management. As summarized in Table 1**,** the system performs efficiently under varying wind speeds and load conditions, showcasing its ability to regulate voltage, mitigate harmonics, and maintain grid stability, all while adhering to IEEE standards. Overall, the proposed system demonstrates strong potential for enhancing grid stability and power quality, making it a viable solution for renewable energy integration while addressing the challenges of power quality in wind energy applications.

Table 1: Summary of the system performance

Test Case	Wind Speed (m/s)	Load Condition at PCC	PMSG Rotor Speed (rad/s)	Grid Current THD (%)	Load Current THD (%)	DC Link Voltage (V)	Grid Voltage (V)	Unity Power Factor Operation	Grid Neutral Current
Case 1	9	Fixed Load	19.6	3.66	16.09	900	415	Yes	Near Zero
	11	Fixed Load	23.9	3.55	16.09	900	415	Yes	Near Zero
Case 2	11	Sudden Reduction	23.9	2.47	12.69	900	415	Yes	Near Zero

V. CONCLUSIONS

This paper has demonstrated the effectiveness of a grid-connected PMSG–WECS with integrated DSTATCOM functionality for enhancing grid power quality. Real-time simulations confirmed the system's capability to maintain stable grid voltage, reduce harmonic distortion, and ensure unity power factor under varying wind speeds and load conditions. The control strategy, combining field-oriented vector control for PMSG and indirect current control for grid-side VSC, enabled efficient power transfer and harmonic compensation. By maintaining the THD of grid-injected currents within IEEE standards (<5%), the system proves its potential for seamless integration into modern power grids. This approach offers a practical and reliable solution for improving grid stability and power quality in wind energy applications.

APPENDIX

Rated wind turbine power	:	$P_m = 7.68\,\text{kW}$	PM flux	:	$\lambda_m = 2.6\,\text{Wb}$
Wind turbine blade radius	:	$R = 2.6\,\text{m}$	System Inertia	:	$J = 1.0\ \text{kg-m}^2$
Optimal TSR	:	$\lambda_{opt} = 5.66$	Rated VSC capacity	:	$S_{VSC} = 10\,\text{kVA}$
Power coefficient	:	$C_{p\max} = 0.4412$	DC link capacitance	:	$C = 2400\,\mu\text{F}$
Rated wind speed	:	$V_\omega = 11\,\text{m/s}$	DC link voltage	:	$V_{DC} = 900\,\text{V}$
Air density	:	$\rho = 1.229\ \text{kg/m}^2$	Grid voltage (r.m.s.)	:	$V_{LL} = 415\,\text{V}$
PMSG stator resistance	:	$R_s = 1.4\,\Omega$	Grid frequency	:	$f = 50\,\text{Hz}$
PMSG stator inductance	:	$L_s = 5.8\,\text{mH}$	Coupling resistance	:	$R_g = 1.5\,\Omega$
PMSG poles	:	$P = 12$	Coupling inductance	:	$L_g = 27.5\,\text{mH}$

ACKNOWLEDGMENT

The authors sincerely thank the Power & Energy Research Centre (PERC) for granting access to their real-time simulation facility, which played a vital role in the successful completion of this research.

REFERENCES

[1] F. Zishan, et al., "Sustainability of the permanent magnet synchronous generator wind turbine control strategy in on-grid operating modes," *Energies*, vol. 16, no. 10, p. 4108, 2023.

[2] Y. Errami, A. Obbadi, and S. Sahnoun, "Dynamic performance analysis of grid-connected PMSG based on nonlinear control," *Int. J. Ambient Energy*, vol. 43, no. 1, pp. 4675–4682, 2021, doi: 10.1080/01430750.2021.1919551.

[3] R. Sadiq, Z. Wang, C. Y. Chung, C. Zhou, and C. Wang, "A review of D-STATCOM control for stability enhancement of power systems with wind/PV penetration: Existing research and future scope," *Int. Trans. Electr. Energy Syst.*, vol. 31, no. 11, pp. 1–27, 2021, doi: 10.1002/2050-7038.13079.

[4] S. Shukla, K. Sahay, and D. K. Tiwari, "Improvement of power quality of grid-connected wind energy system using D-STATCOM," *AIP Conf. Proc.*, vol. 2640, no. 1, p. 020018, Sept. 2022, doi: 10.1063/5.0117794.

[5] S. M. Tripathi and P. J. Barnawal, "Design and Control of a D-STATCOM for Non-Linear Load Compensation: A Simple Approach," *Electr. Control Commun. Eng.*, vol. 14, no. 2, pp. 172–184, 2018, doi: 10.2478/ecce-2018-0021.

[6] M. K. K. Prince, M. T. Arif, A. Gargoom, A. M. T. Oo, and M. E. Haque, "Modeling, Parameter Measurement, and Control of PMSG-based Grid-connected Wind Energy Conversion System," *J. Mod. Power Syst. Clean Energy*, vol. 9, no. 5, pp. 1054–1065, 2021, doi: 10.35833/MPCE.2020.000601.

[7] V. K. Govil, K. Sahay, and S. M. Tripathi, "Enhancing power quality through DSTATCOM: a comprehensive review and real-time simulation insights," *Electr. Eng.*, 2024, doi: 10.1007/s00202-024-02409-5.

[8] S. M. Tripathi, A. N. Tiwari, and D. Singh, "Optimum design of proportional-integral controllers in grid-integrated PMSG-based wind energy conversion system," *Int. Trans. Electr. Energ. Syst.*, vol. 26, pp. 1006–1031, 2016, doi: 10.1002/etep.2120.

[9] H. Shutari, T. Ibrahim, N. B. MohdNor, Y. Z. Alharthi, and H. Abdulrab, "Control approaches of power electronic converter interfacing grid-tied PMSG-VSWT system: A comprehensive review," *Heliyon*, vol. 10, no. 12, p. e32032, 2024, doi: 10.1016/j.heliyon.2024.e32032.

[10] D. V. N. Ananth and L. V. S. Kumar, "Power Quality Enhancement in Distribution Networks with Pmsg Renewable Energy Integration with Nonlinear Loads Using Advanced Intelligent Controllers," *SSRN*, 2024, doi: 10.2139/ssrn.4939957.

[11] H. Salime, B. Bossoufi, Y. El Mourabit, and S. Motahhir, "Robust Nonlinear Adaptive Control for Power Quality Enhancement of PMSG Wind Turbine: Experimental Control Validation," *Sustainability*, vol. 15, no. 939, 2023, doi: 10.3390/su15020939.

[12] G. Mayilsamy, K. Palanimuthu, R. Venkateswaran, R. P. Antonysamy, S. R. Lee, D. Song, and Y. H. Joo, "A Review of State Estimation Techniques for Grid-Connected PMSG-Based Wind Turbine Systems," *Energies*, vol. 16, no. 634, 2023, doi: 10.3390/en16020634.

[13] Z. Zhang, X. Zhao, L. Fu, and M. Edrah, "Stability and Dynamic Analysis of the PMSG-Based WECS With Torsional Oscillation and Power Oscillation Damping Capabilities," *IEEE Trans. Sustain. Energy*, vol. 13, no. 4, pp. 2196–2210, Oct. 2022, doi: 10.1109/TSTE.2022.3188442.

[14] T. Qu, et al., "Damping torque coefficient analysis of PMSG-based WT with VSG control considering wind turbine dynamics," *IET Gener. Transm. Distrib.*, vol. 17, no. 2, pp. 367–379, 2023.

[15] S. M. Tripathi, A. N. Tiwari, and D. Singh, "Grid-integrated permanent magnet synchronous generator based wind energy conversion systems: A technology review," *Renew. Sustain. Energy Rev.*, vol. 51, pp. 1288–1305, 2015, doi: 10.1016/j.rser.2015.06.060.

[16] A. Radwan, et al., "Grid-Forming Voltage-Source Converter for Hybrid Wind-Solar Systems Interfacing Weak Grids," *IEEE Open J. Power Electron.*, 2024.

[17] D. Kumar and K. Chatterjee, "A review of conventional and advanced MPPT algorithms for wind energy systems," *Renew. Sustain. Energy Rev.*, vol. 55, pp. 957–970, 2016, doi: 10.1016/j.rser.2015.11.013.

[18] M. A. Rahman, "Analysis of current controllers for voltage-source inverter," *IEEE Trans. Ind. Electron.*, vol. 44, no. 4, pp. 477–485, 1997, doi: 10.1109/41.605621.

[19] S. M. Tripathi, U. P. Singh, S. Singh, N. K. Rai, and A.K. Srivastava, "Hardware-in-the-loop testing of grid-tied PMSG-based wind power generation system with optimum PI parameters," *e-Prime - Adv. Electr. Eng., Electron. Energy*, vol. 5, p. 100282, 2023, doi: 10.1016/j.prime.2023.100282.

[20] R. Aljarrah, B. B. Fawaz, Q. Salem, M. Karimi, H. Marzooghi, and R. Azizipanah-Abarghooee, "Issues and Challenges of Grid-Following Converters Interfacing Renewable Energy Sources in Low Inertia Systems: A Review," *IEEE Access*, vol. 12, pp. 5534–5561, 2024, doi: 10.1109/ACCESS.2024.3349630.

[21] S. Rahman, S. Li, H. S. Das, X. Fu, H. Won, and Y. K. Hong, “Exploring Dynamic P-Q Capability and Abnormal Operations Associated with PMSG Wind Turbines,” *Energies*, vol. 16, no. 4116, 2023, doi: 10.3390/en16104116.

[22] C. Zhao, W. Chai, B. Rui, and L. Chen, “Analysis of Sub-Synchronous Oscillation of Virtual Synchronous Generator and Research on Suppression Strategy in Weak Grid,” *Energy Eng.*, vol. 120, no. 11, pp. 2683–2705, 2023, doi: 10.32604/ee.2023.029620.

[23] P. K. Goel, B. Singh, S. S. Murthy, and N. Kishore, “Isolated wind-hydro hybrid system using cage generators and battery storage,” *IEEE Trans. Ind. Electron.*, vol. 58, no. 4, pp. 1141–1153, 2011, doi: 10.1109/TIE.2009.2037646.

[24] S. M. Tripathi, A. N. Tiwari, and D. Singh, "Controller design for a variable-speed direct-drive permanent magnet synchronous generator-based grid-interfaced wind energy conversion system using D-partition technique," *IEEE Access*, vol. 5, pp. 27297-27310, 2017, doi: 10.1109/ACCESS.2017.2775250.

[25] V. S. K. V. Harish and A. V. Sant, "Grid integration of wind energy conversion systems," in *Alternative Energy Resources*, vol. 99, P. Pathak and R. R. Srivastava, Eds., Cham: Springer, 2020, doi: 10.1007/698_2020_610.

[26] M. Singh, V. Khadkikar, and A. Chandra, "Grid synchronisation with harmonics and reactive power compensation capability of a permanent magnet synchronous generator-based variable speed wind energy conversion system," *IET Power Electronics*, vol. 4, no. 1, pp. 122–130, 2011, doi: 10.1049/iet-pel.2009.0132.